AERODYNAMIC DESIGN OF SWEPT WINGS AND BODIES FOR TRANSONIC SPEEDS

By R. C. Lock and E. W. E. Rogers

Aerodynamics Division, National Physical Laboratory
Teddington, Middlesex, United Kingdom

1. INTRODUCTION

For many years the concept of sweepback has been used with beneficial effect in raising the economical cruising speed of subsonic aircraft. As we try to extend this speed still further it is necessary at the same time to increase the angle of sweep and, usually, to decrease the aspect ratio, and it becomes more and more difficult to obtain the full theoretical benefits of sweepback, largely because of adverse effects on the root and tips of the wings; in the transonic speed range these adverse effects are liable to cover the whole span unless special measures are taken. It is the purpose of the present paper to outline some of the principal ways of remedying these defects and of extending the speed range in which sweptback wings may usefully be used; cruise Mach numbers up to about 2 are envisaged, and in fact the upper limit may well be set by structural and low-speed aerodynamic considerstions rather than by the cruising aerodynamics[1].

The physical basis of the method is to shape the wings and fuselage together in such a way that the chordwise pressure distribution on the wings at the design condition should be independent of spanwise position, and that the component of local Mach number normal to the fully swept isobars thus obtained should be everywhere less than one. Such an ideal state of affairs is sketched in Fig. 1. In this way it should be possible to ensure that the flow over the wings is free from shock waves and that the wing wave drag is low. If the cruising Mach number exceeds the critical for a low-drag body of revolution having the same length and volume as the wing-fuselage combination considered, some overall wave drag is of course inevitable, and the same is true at all supersonic speeds with regard to wave drag due to lift. It is not claimed that the present methods will lead to strict "minimum wave drag" configurations in any ideal mathe-

matical sense, but it is felt that, because the type of flow specified is a physically reasonable one, it should be possible to realize it in practice.

Provided that the wings are not too highly tapered, the flow over them will then be equivalent in many ways to that over an infinite yawed wing having the same basic pressure distribution and sweepback ϕ. The first step in the design process must thus be to consider the two-dimensional

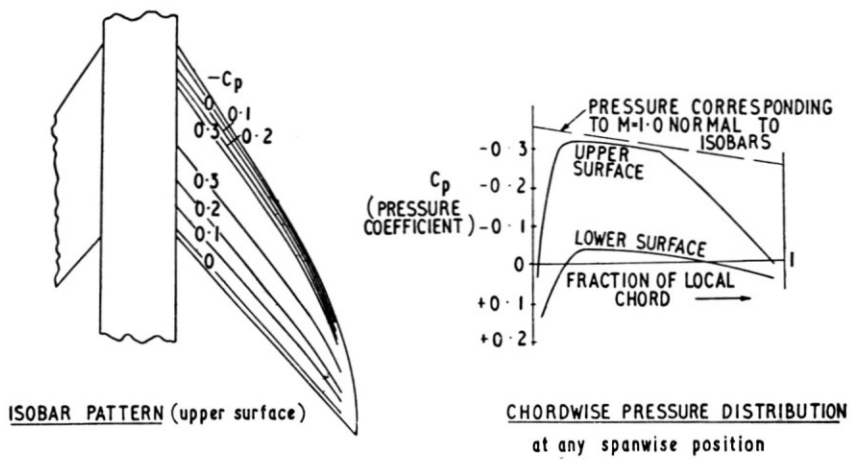

FIG. 1. An ideal wing pressure distribution.

flow, at a Mach number $M_0 \cos \phi$ obtained by resolving the freestream Mach number M_0 normal to the wing leading edge, past a normal section of the yawed wing; this will have an incidence $\alpha \sec \phi$ and thickness/chord ratio $\tau \sec \phi$, and give a lift coefficient $C_L \sec^2 \phi$, where α, τ and C_L refer to the yawed wing.* It should therefore be possible to incorporate the refinements in two-dimensional design methods described by Pearcey[2] into a highly swept configuration.

The tools that enable us to attempt this include choice of the wing planform, shaping the fuselage and warping the wings, particularly near the root and tips. Before going on to describe these techniques in detail, it is instructive to consider briefly the physical nature of the transonic flow about a typical swept wing that has not been treated in this way, so as to emphasize some of the phenomena that we wish to avoid in a more refined design. We shall also present some recent experimental evidence of the equivalence between yawed and two-dimensional wings, referred to above.

* C_L and τ will be the same as for the actual finite configuration but α will in general be different.

2. THE FLOW DEVELOPMENT ABOUT UNTREATED SWEPTBACK WINGS

In discussing briefly the general flow development[3] with stream Mach number, it is convenient to consider a simple, plane wing whose planform, which may be tapered, is defined by straight lines. At moderate subsonic speeds and if the lift is not large, an important effect of the sweep is to move the loading forward at the tip, and rearward at the root, compared with

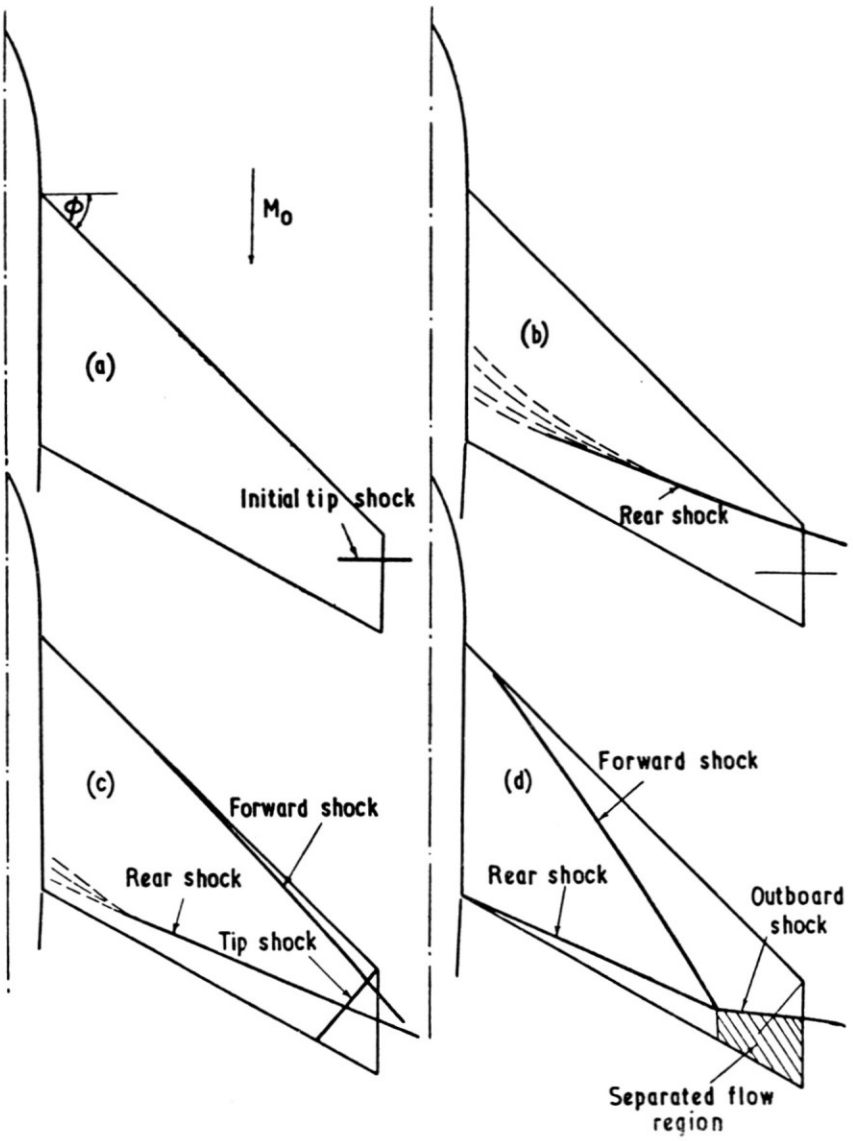

FIG. 2. Flow development about simple swept-back wing with increasing stream Mach number.

the corresponding yawed wing; the highest local velocities, and hence the first appearance of supersonic flow, occur in the tip region. Unfortunately, the isobars near the wing tip lose much of their sweep and hence the supersonic flow is associated with a shock wave (the initial tip shock). This is comparatively weak and lies almost normal to the oncoming stream; though limited in spanwise extent from the wing tip (Fig. 2(a)), it can extend to considerable distances above and below the wing. The initial tip shock moves rearwards over the wing surface as the stream Mach number is further increased, but its influence on the wing is limited by the appearance of a second shock (the rear shock) which usually forms at about the same time. The rear shock rapidly develops to affect a large part of the wing span and in particular the flow just ahead of the initial tip shock (Fig. 2(b)).

The rear shock may be regarded as associated primarily with conditions at the wing root; the effect of the section thickness is to turn the local flow inboard, an effect which near the root must be constrained by the body surface and the need for flow symmetry at the centre line. The inward-turning flow is therefore straightened by a compression system propagating outward from the root which coalesces on the outer part of the wing to form a shockwave.

With increasing stream Mach number, the rear shock moves aft more rapidly than the initial tip shock which is overtaken and disappears. At the same time, the region of diffuse recompression at the inboard side of the rear shock contracts as the shock spreads towards the root. At a sufficiently high Mach number the rear shock reaches the trailing edge and this condition will be achieved earlier for a delta wing than, say, for an untapered wing with the same leading-edge sweep. At some stage, the rear shock may become sufficiently strong to cause boundary-layer separation, with a consequent modification of both the surface flow behind the shock and the overall wing characteristics. The development of the rear shock, particularly over the inner part of the wing, may be influenced by the shock which forms on the central body at high subsonic speeds and in certain cases (e.g. a highly curved body and a thick wing) a complex interaction may take place.

The high local flow velocities present close to the leading edge over the outer part of the wing lead to large chordwise pressure gradients in that region and, at a sufficiently high incidence, to flow separation at the leading edge. This starts near the tip and spreads inboard with increasing incidence. For leading-edge sweeps greater than about 30°, the separated flow rolls up to form a partspan vortex lying obliquely across the wing. There is usually little effect of stream Mach number on the onset and development of the leading-edge separation, except when the leading

edge is very blunt. At high subsonic stream speeds however, the vortex may interact with, and be distorted by, the rear shock lying over the after part of the wing. Above a certain stream Mach number the flow changes in type; the leading-edge separation is suppressed, the flow passes smoothly around the leading edge and passes through a shockwave (the forward shock) which appears to originate close to the leading edge at some span-

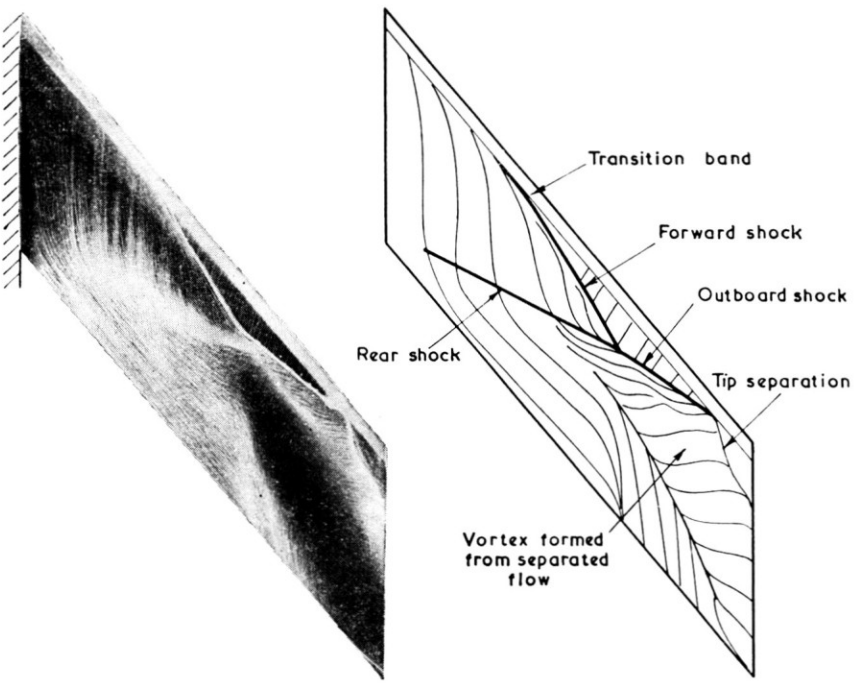

FIG. 3. Complete flow pattern on 50° swept wing: $M = 0{\cdot}95$, $\alpha = 10°$.

wise position and to turn back over the wing surface outboard of this station (Fig. 2(c)). The forward shock is in fact the boundary of disturbances from the inboard part of the wing leading edge, which because of the higher local supersonic Mach number, propagate over the outer wing in a direction more highly swept than the leading edge.

The Mach number component normal to the leading edge ($M_0 \cos\phi$) for which the flow attachment occurs varies considerably, depending on the wing sweep and more particularly on the leading edge profile; in general the component has a value between about 0·55 and 0·90.

As the stream Mach number is increased beyond that necessary for flow attachment, the forward shock moves inboard and rearward (but with almost constant geometric sweep) and hence at some stage intersects the rear shock. Outboard of this intersection a strong shock forms (the outboard

shock) which frequently induces a severe flow separation, even though the flow is attached behind both the forward and rear shock (Fig. 2(d)). When separation is present behind either of these shocks, a vortex tends to form and the associated outflow modifies the flow structure outboard and becomes an important factor in the ultimate breakdown in the attached type of leading-edge flow over the wing. Separation then takes place

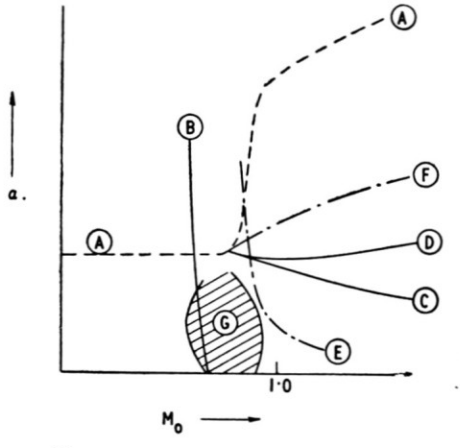

Ⓐ Leading-edge separation
Ⓑ Appearance of rear shock
Ⓒ Appearance of forward shock
Ⓓ Appearance of outboard shock, with separation to rear
Ⓔ Separation behind rear shock
Ⓕ Separation behind forward shock
Ⓖ Zone in which initial tip shock exists

Fig. 4. Typical boundary diagram for wing of about 50° sweep.

along almost the entire leading edge; the shockwaves no longer have a direct influence upon the surface pressures, which are dominated by a large part-span vertex as at lower, and subsonic, stream speeds.

Many of the features described briefly above are shown in the surface-film pattern of Fig. 3, obtained at a Mach number of 0·95. Typical boundaries for a wing of about 50° sweep are included as Fig. 4.

Complex flows similar to Fig. 3 are largely due to the three-dimensional nature of the wing flow and hence to the dominance of the root and tip influence at transonic speeds. The root affects the flow strongly behind the forward shock (which therefore indicates the limit of the root influence) and the flow in this region is partly conical in character. The tip influence at transonic speeds is delineated by small disturbance from near the tip leading edge (the tip shock). Ahead of the forward, outboard

and tip shocks the flow is almost free from constraint effect due to the finite span of the wing and has therefore marked two-dimensional characteristics. The extent of this zone depends on the shock positions which are in turn dependent on wing planform, section incidence and stream Mach number. By making the aspect ratio of the wing very large, or by deliberately attempting to reduce the root and tip influence on a given wing, flow

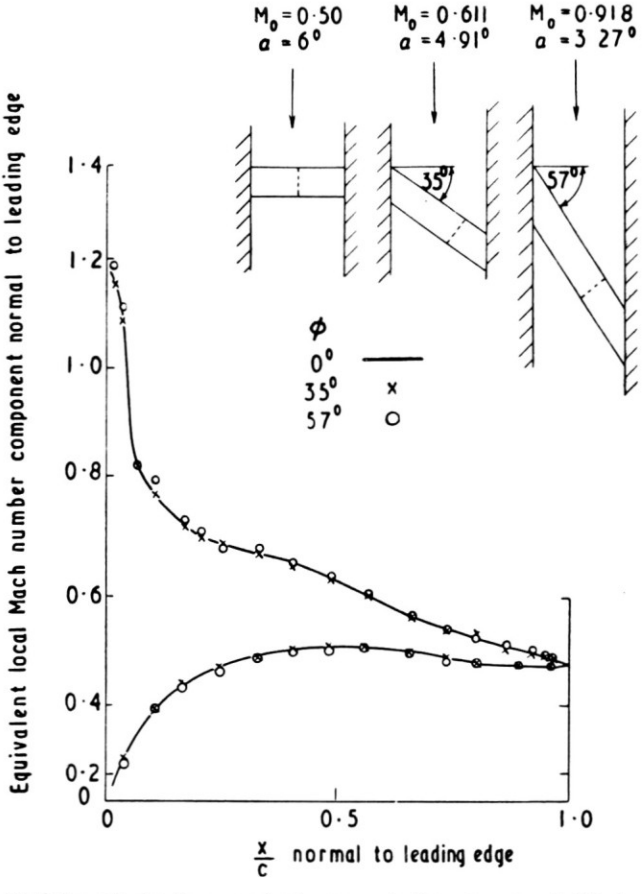

FIG. 5. Validity of simple sweepback concept for component Mach number of 0·5 normal to leading edge. 10% thick aerofoil section; no treatment of model–wall junctions.

can be obtained over a larger portion of the wing which closely resembles that postulated in the simple sweepback theory and which is so highly desirable.

Many attempts have been made to show the relationship between swept-wing flow and that on the equivalent two-dimensional section at a component Mach number $M_0 \cos\phi$. The precision of this relationship is com-

paratively easy to demonstate when $M_0 \cos\phi$ is not large, as in Fig. 5. At higher values it is extremely difficult to minimize the effects of the finite wing aspect ratio. Recent experiments at the NPL however have given satisfactory results, surface pressures, separation boundaries and shock position correlating well on the basis of the simple sweep theory. Typical results are included as Fig. 6. Much of the success must be attrib-

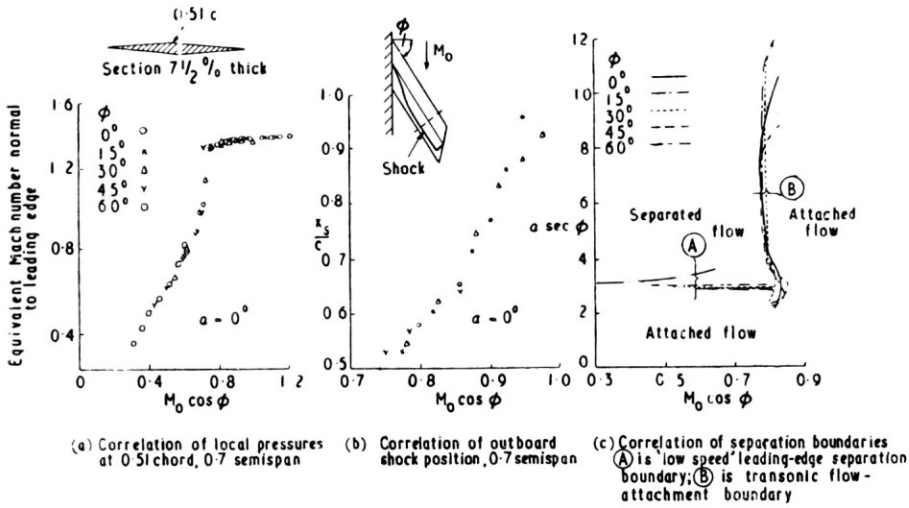

FIG. 6. Application of simple sweepback theory to results from plane half-wing with double-wedge section and variable sweep. No root treatment.

uted to the fact that for this particular wing profile ($7\frac{1}{2}\%$ thick symmetrical double wedge) a shock similar in nature to the forward shock originates from the ridge line at mid-chord; except at high incidence the local velocities in the leading-edge region are relatively low. A large part of the wing behaves as a yawed two-dimensional section and the zone subject to a severe root influence is small. The double-wedge section, though not suitable for real swept back wings, is valuable nevertheless in allowing the underlying structure and unity of swept-wing flow to be demonstrated.

In practice, the wing section is chosen largely from two-dimensional considerations (such as a high drag-rise Mach number) but since the wing aspect ratio is usually too small to allow the natural attrition of root and tip influences to take place, judicious changes in the wing planform, profile and root contour are necessary to modify the flow about the untreated wing, replacing it by one close to the yawed-wing model and thus approaching the optimum aerodynamic design. Methods that are available for effecting such changes will now be considered.

3. WING PLANFORM DESIGN

As pointed out in the previous section, swept wings with conventional straight-edged planforms have two principal defects in the transonic speed range. The first is that, particularly when the planform is highly tapered, the suction peaks near the leading edge of an uncambered wing at incidence increase rapidly towards the tips, and the associated high values of the local Mach number soon exceed the critical value normal to the isobars, so that shockwaves form (Fig. 2) prematurely in this region. The second is that the sharp corner at the tip leading edge produced a "tip shock" which, though seldom strong enough in itself to cause boundary layer separation or high drag, is instrumental in unloading the rear part of the wing near the tip and thereby reducing its efficiency as a lifting surface. Fortunately, it is possible in principle to attend to both these defects together by suitable design of the wing planform.

The suction peaks which occur in a real flow are associated in linearized theory with the singularity in the local loading at the leading edge. Using the notation of Fig. 7, we can define the strength σ of this singularity by

$$\frac{l}{4\alpha} \sim \frac{\sigma}{\sqrt{2\xi}} \quad \text{as} \quad \xi \to 0 \tag{1}$$

where l is the difference in pressure coefficient between the upper and lower surface of a plane wing at incidence α and ξ is the local chordwise position. In the simple form taken by lifting surface theory at $M = 1$[4,5] it can be shown that, downstream of the Mach line from the root trailing edge ($x = 1$),

$$\sigma = H\sqrt{1-k^2}\sqrt{\frac{y\,\mathrm{d}y}{c\,\mathrm{d}x_l}} \tag{2}$$

where $k = \dfrac{x_l(\eta)-1}{y\tan\phi_t}$, c is the local chord and $H(x_l)$ is the function defined by Mangler[4], which is determined, through a rather complicated integral equation, from the shape of the leading edge upstream of $x = x_l$; for $x < 1$, $H\sqrt{1-k^2}$ is to be replaced by 1. For a highly tapered wing with straight leading and trailing edges $H\sqrt{1-k^2} = 1$ throughout, and the leading edge singularity takes the form shown in Fig. 7; the rapid increase towards the wing tip is clearly seen.

In order to avoid this increase, we first choose the initial shape of the leading edge, upstream of $x = 1$, in an arbitrary way—usually straight with a suitable amount of basic taper—and then downstream of $x = 1$, fix the strength σ of the singularity at the constant value σ (cf. Fig. 7). Equation (2) then becomes an integro-differential equation for $x_l(y)$, and

thus the desired shape of the leading edge can, in principle, be found. Details are given in ref. 6 of an approximate method of doing this which should be of adequate accuracy for most practical purposes. Keeping the trailing edge straight and at a fixed angle of sweepback ϕ_t, several families of planforms, each of varying aspect ratio, have been found[6]. Three

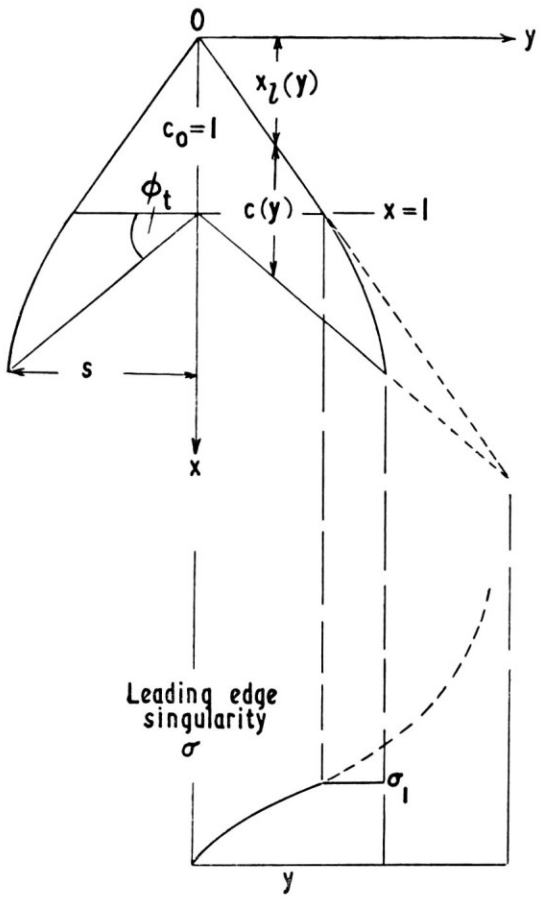

FIG. 7. Typical wing planform and variation of leading edge singularity.

typical members of the simplest and most useful family are shown in Fig. 8. Variation of the basic trailing edge sweep can be introduced by multiplying all transverse (y) dimensions by a constant, keeping all longitudinal (x) dimensions fixed.

An important feature of these planforms is that, once the leading edge singularity is held constant and independent of spanwise position, so also to a large extent is the whole shape of the chordwise loading curves. This is illustrated in Fig. 9, which shows chordwise loading curves at various

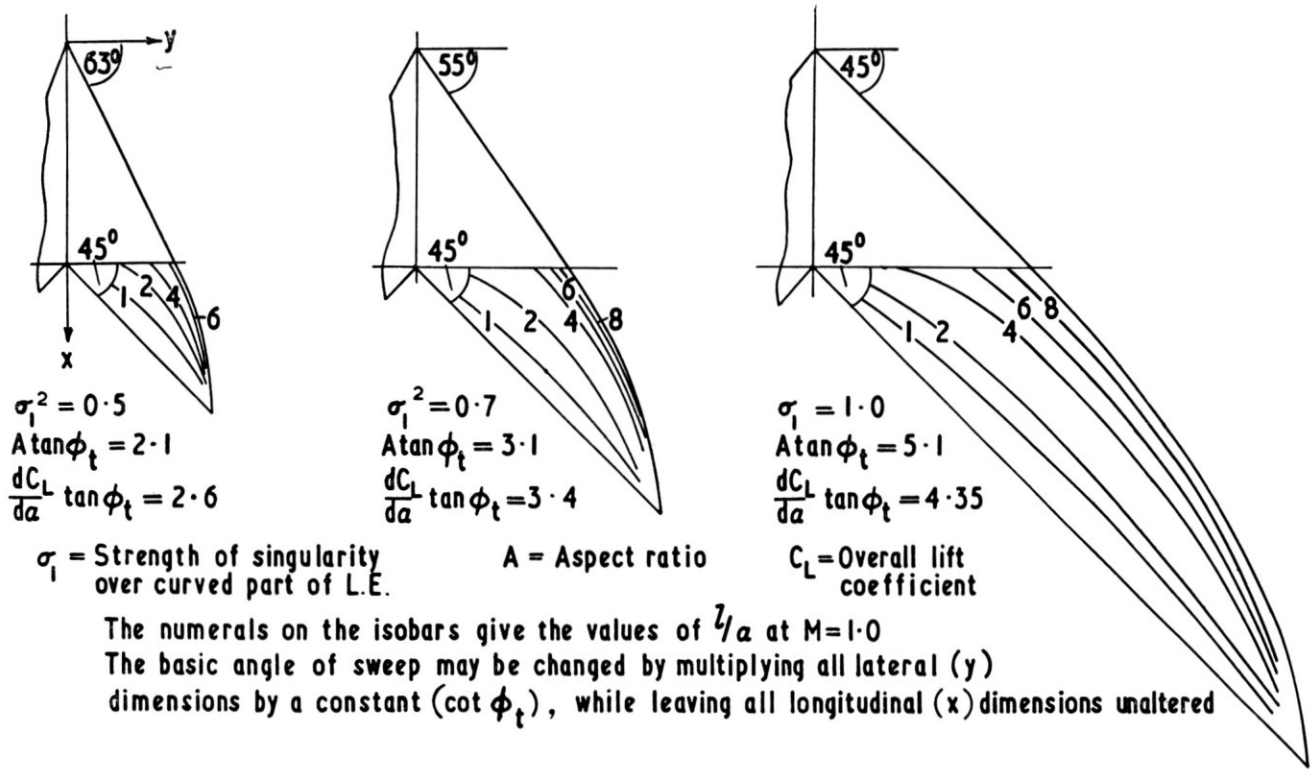

FIG. 8. Typical wing planforms.

spanwise position for one of the wings (C) of Fig. 8. As a result, the theoretical isobars (for a thin plane wing) follow closely the lines of constant chordwise position in the tip region and are fully swept there (see Fig. 8), while there is no loss of loading anywhere on the wing. The local lift coefficient varies little across the span, and since the distribution of chord $c(y)$ is not far from elliptical, the spanwise loading curves give favourable theoretical induced drag factors, not exceeding 1·05 in any of the examples given.

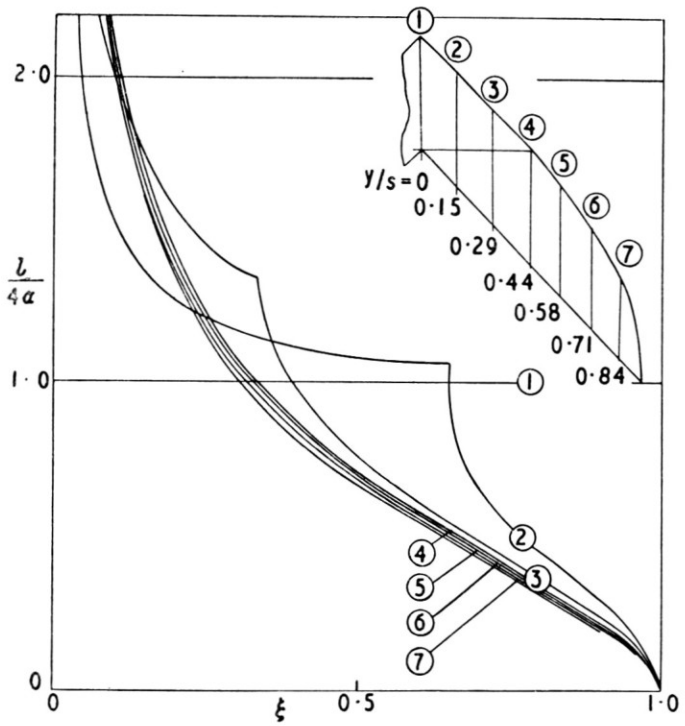

FIG. 9. Chordwise loading curves (planform C of Fig. 8).

Although the adoption of a planform designed in this way should by itself be most efficaceous when the wing is uncambered, it is not in fact proposed to use an uncambered wing; as described later in Section 5, it is essential to apply suitable camber, twist and fuselage shaping before the full benefits of wing design can be obtained, and this can in principle be done whatever the wing planform, at least for one particular design incidence or lift coefficient. The special planforms will still have two advantages, however; in off design conditions they should help retain a satisfactory loading and isobar pattern in the tip region, and they will also reduce the amount of variation in camber and twist required there.

4. THICKNESS EFFECTS

Having chosen the wing planform and basic section (cf. ref. 2), it is now necessary to consider the detailed shaping of the wing and fuselage in order to obtain the full benefit of the wing sweep and section design. At the present stage it is necessary to use linearized theory for most of the work, and it is therefore convenient to split the design process into two parts, dealing separately with the effects of thickness (at zero incidence) and lift.

The problem of designing a symmetrical wing-fuselage combination at zero incidence so as to minimize the wave drag has of course been studied for many years, and two apparently distinct methods of approach

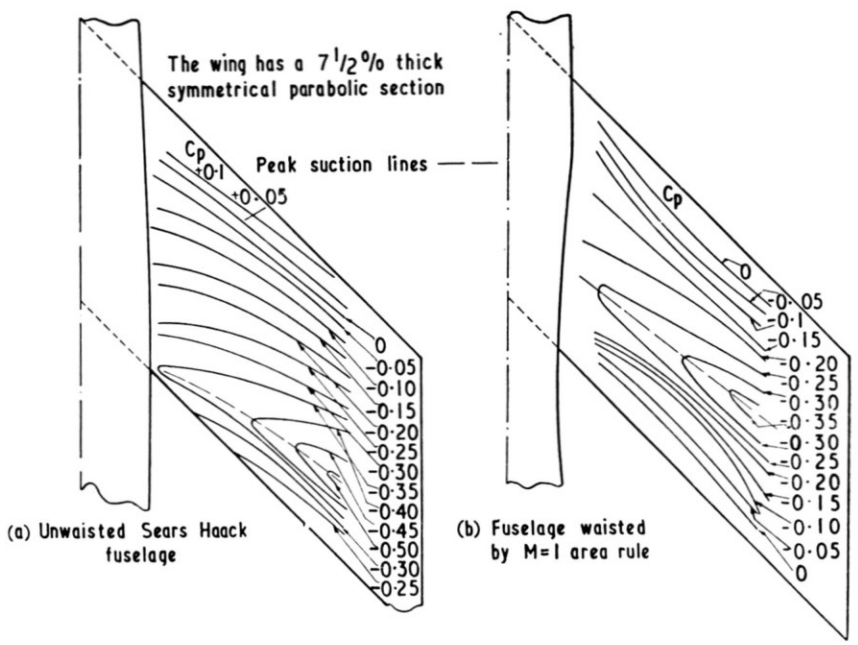

FIG. 10. Effect of area rule waisting on isobar patterns. N.P.L. experiments: $\alpha = 0$ $M = 1{\cdot}0$.

have been evolved. The first is that of Whitcomb[7,8], who from considerations of the overall flow pattern and forces developed the Area Rule and its more recent extensions. The second, due to Küchemann and his collaborators[9], is based on considerations of the details of the flow and pressure distribution, particularly near the wing-fuselage junction; the fundamental idea is the same as that of the present paper, to shape the fuselage and if necessary the wing as well so as to achieve a straight, fully swept, sub-critical isobar pattern right up to the junction. This idea was first put forward for high subsonic speeds[9], but the principle is equally

applicable at sonic or supersonic speeds; an extension of the design method to the latter case has recently been developed by Bazley (unpublished). At present, however, the method is only able to deal with the pressure at the actual junction (or at most at one or two other discrete stations along the wing), and also suffers from the use of some undesirable approximations with regard to the wing-fuselage interference. In spite of these limitations it has proved successful in practice both at subsonic and low supersonic (up to $M = 1{\cdot}2$) speeds.

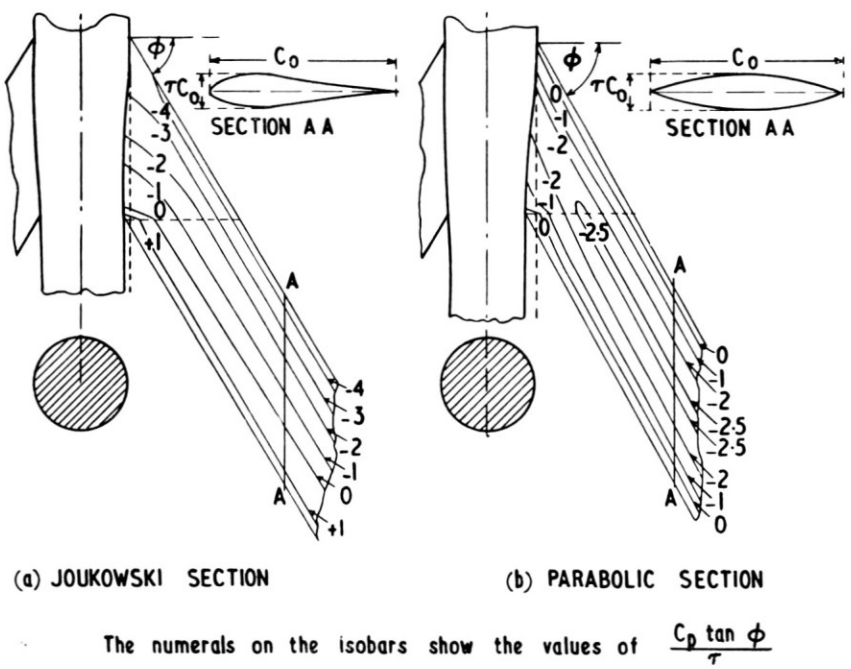

FIG. 11. Theoretical isobar patterns: $M = 1$, $\alpha = 0$ for wing-fuselage combinations waisted according to the sonic area rule.

Although the two methods appear at first sight entirely different, it is now clear that there is in fact a considerable measure of agreement between them; this is particularly true when the basic wing thickness and sweep are such that the equivalent infinite yawed wing would be subcritical—that is, below the drag rise—and this is just the case where the area rule is most successful. For example, Fig. 10 shows some results of recent (unpublished) tests at the National Physical Laboratory on a simple wing-fuselage combination at zero incidence, with and without fuselage waisting according to the sonic area rule; the improvement in the isobar pattern produced by the waisting can be clearly seen. A similar conclusion was reached theoretically by Byrd[10], who calculated the pres-

sure distribution at $M = 1$ on an infinite swept wing mounted on a long circular cylinder, again waisted according to the sonic area rule; the isobar patterns for two widely different wing section (Fig. 11) are very satisfactory. Further theoretical and experimental evidence on this point is given in ref. 11.

It therefore seems evident that the ideal solution to the problem would combine the two methods. Thus the overall area distributions must be such as to give as low a value as possible for the total wave drag, according to the area rule at the design Mach number; while the detailed shaping of the wing and fuselage must at the same time yield the desired isobar pattern. This process would clearly involve appropriate variations in the wing thickness distribution and in the cross-sectional shape of the fuselage. The former approach has been used with success at subsonic speeds by Haines[12], without the need for any fuselage shaping; it must be emphasized that at higher speeds this can no longer be sufficient in itself because of the necessity of achieving satisfactory overall area distributions. The latter approach—combining the area rule with fuselage cross-section shaping to give the desired junction pressure distribution—has been tried by McDevitt[11], but he was not successful in obtaining any additional reduction in drag by this method. Thus there is scope for further developments in this field; though in the meantime it can safely be said that either the area rule or the Küchemann–Bagley method does give a close approximation to the desired conditions, at least in the transonic speed range.

5. LIFTING EFFECTS

The final stage in the design process is to continue the shaping of the wing and fuselage so that, at the design lift coefficient, the desired type of pressure distribution is achieved on the wings. In order to do this, we first choose a suitable chordwise loading distribution

$$\Delta C_p = l(\xi) \tag{3}$$

and apply it at all spanwise positions to the wing planform, suitably continued through the fuselage. Following the method of Richardson and Parry[13], it is then possible to calculate the complete flow field due to this loading distribution. Thus the velocity perturbation u is given (cf. ref. 14) by $u = \text{grad } \phi$, where (at supersonic free-stream Mach numbers)

$$\phi(x, y, z) = -\frac{U_0}{4\pi} \int\int \frac{z(x-x_1)\, l(x_1, y_1)\, \mathrm{d}x_1\, \mathrm{d}y_1}{[(y-y_1)^2+z^2][(x-x_1)^2-\beta^2(y-y_1)^2-\beta^2 z^2]^{1/2}} \tag{4}$$

$$l(x, y) \equiv l(\xi)$$

$$\xi = \frac{x-x_l(y)}{c(y)}$$

and

$$\beta = \sqrt{M_0^2 - 1}$$

the integration is to be carried out over all points $(x_1 y_1)$ of the wing planform lying within the Mach forecone of the point(x,y,z).

In particular, we can find the downwash in the mean plane ($z = 0$) of the exposed wing, and thus determine the camber surface of the wing, and we can shape the fuselage so that this also becomes a stream surface

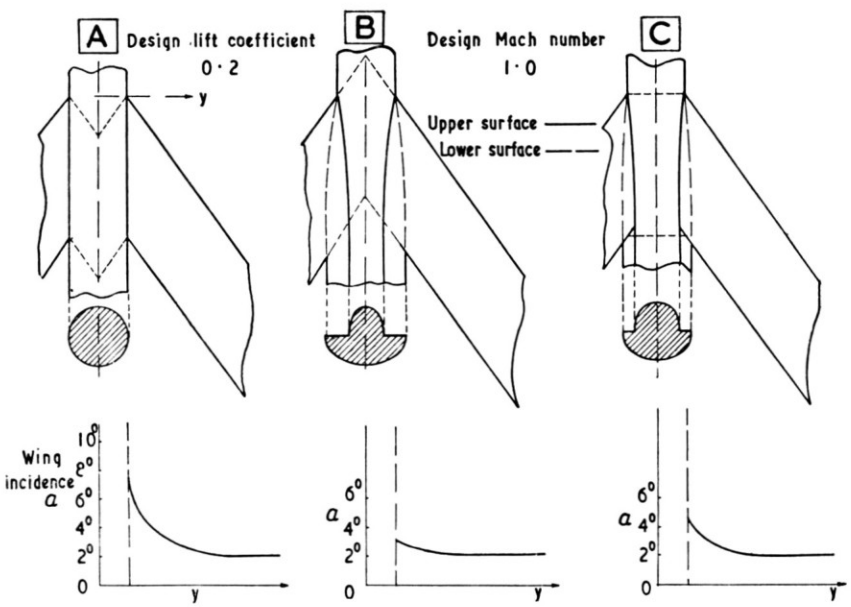

FIG. 12. Asymmetric fuselage shaping and wing twist: effect of alternative planforms.

for the desired loading distribution; the latter calculation may be simplified by replacing the actual fuselage by a mean circular of constant radius R_0, calculating the normal component of velocity induced on it, and hence the required streamwise slope of the fuselage. Since the disturbance potential ϕ due to a planar loading distribution of this type is antisymmetric with respect to z, the sidewash v is also antisymmetric while the upwash w is symmetric. It follows that the resulting fuselage shape is also asymmetric about the wing plane; relative to the original shape determined (as in Section 4) from thickness considerations, more waisting will usually be required above the wing and less below it, the total cross-sectional area remaining the same. A similar scheme, but based on weaker theoretical foundations, has been tried with success by Palmer and others[15], and yet another by Lock and Rogers[16].

The detailed shape of wings and fuselage produced by this process is extremely sensitive, particularly near the wing-fuselage junction, to the way in which the wing planform is assumed to continue through the fuselage. This is illustrated in Fig. 12, which sketches the effect of three possible choices. In the first case (A), little or no additional fuselage shaping is required, but because of the kink in the planform at the fuselage side the downwash in the plane $z = 0$ and therefore the local wing incidence there have a logarithmic infinity. This difficulty can be partially overcome, as suggested by Weber[20], by calculating the downwash at $z = z_t$, where z_t is half the local wing thickness; but the resultant incidences remain very high and change rapidly with y near the junction. At the other extreme (B), where the assumed planform is fully swept up to the centre line, the wing twist is small but the differential waisting required is large. It may in fact be shown that in this case, for a basically untapered wing, the sidewash v at the junction is given by*

$$\frac{v}{U_0} = \mp\frac{1}{4}\tan\phi I(\xi) \begin{pmatrix} - \text{ for } z > 0 \\ + \text{ for } z < 0 \end{pmatrix} \tag{5}$$

so that the required change in the fuselage lateral (y) dimension is

$$\frac{\Delta y}{C} = \pm\frac{1}{4}\tan\phi L(\xi) \tag{6}$$

where

$$L(\xi) = \int_0^{\xi} I(x)\,\mathrm{d}x \tag{7}$$

In particular the "step" in the fuselage at the trailing edge is of width $\frac{1}{2}\,cC_L \tan\phi$, and for a typical design lift coefficient of 0·2 and sweepback 55° this is about one tenth of the wing root chord or half the basic fuselage radius.

A third possibility (C), which is intermediate in every sense between (A) and (B), is to leave the assumed wing planform unswept inside the fuselage. There is still a kink in the planform at the fuselage side, but it is only half as big as in (A), so that the wing twist required is approximately halved while the fuselage indentation is (exactly) half that in case (B). It is suggested that this arrangement may form a practical compromise in many cases, but it is of course possible, by further variation of the planform inside the fuselage in a similar way, to alter the relative amounts of wing twist and fuselage indentation as desired; provided only that the total magnitude of these two alternative devices is adequate to produce the required effect on the flow and pressure distribution.

* This result is independent of Mach number.

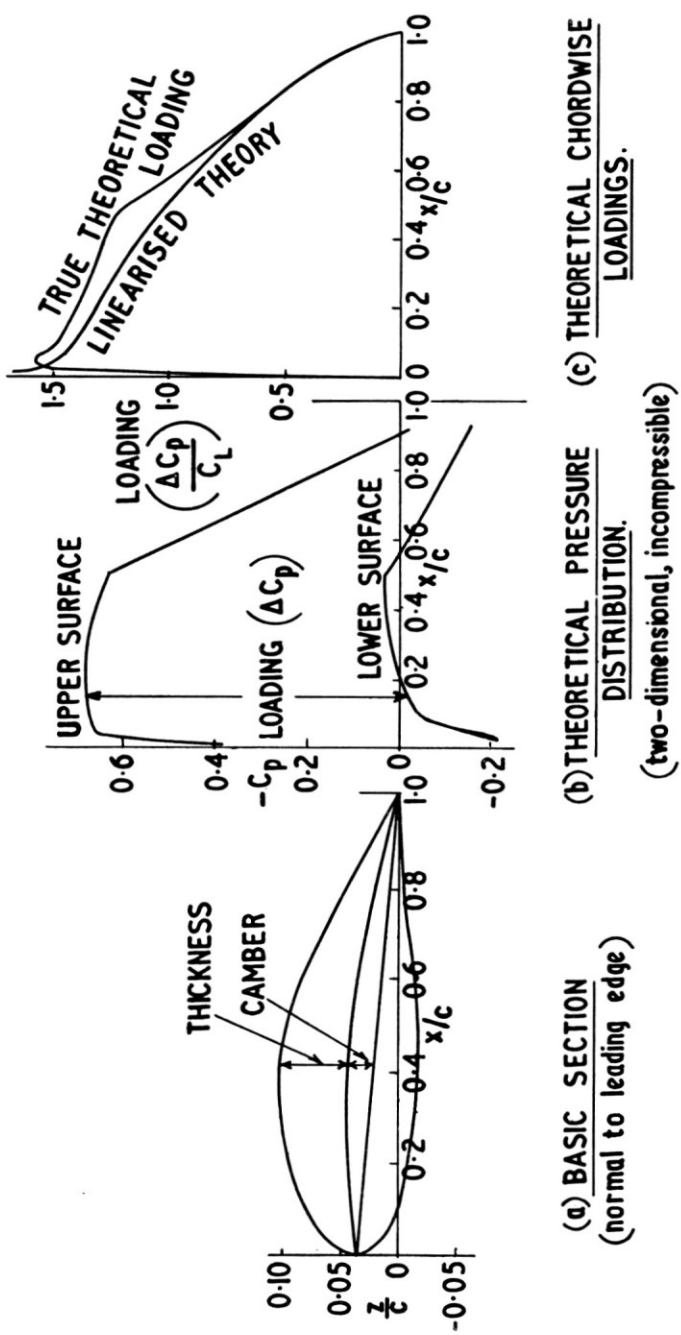

FIG. 13. Steps in swept-wing design.

Calculations of the normal component of velocity induced on the fuselage show that the cross-sections of the upper and lower halves are approximately elliptical. The values of the downwash in the vertical plane of symmetry ($y = 0$) suggest that the fuselage should be cambered as shown in Fig. 13 for a typical case; but in practice there seems no reason to unload the forward part of the fuselage in this way, and a uniform fuselage incidence would probably be adopted.

The choice of the chordwise loading $l(\xi)$ is also of great importance, but at present it is no means clear how this should best be done in general. But when the wing is basically untapered over much of the span, the following procedure is suggested. Having chosen our basic two-dimensional

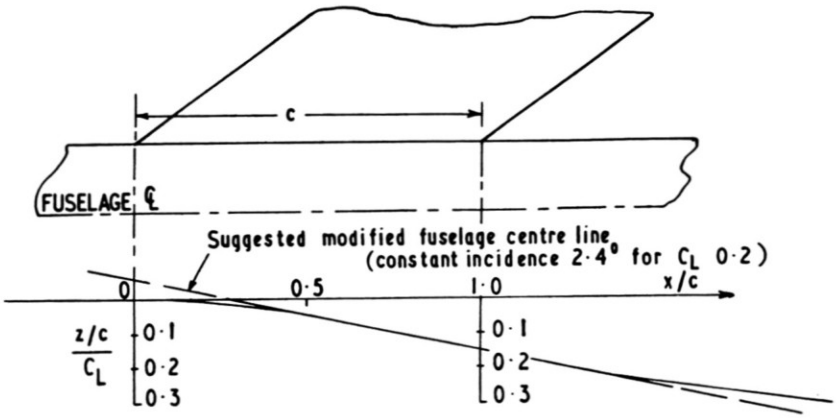

FIG. 14. A typical fuselage camber line.

section as explained in (2), we use its camber line to calculate a loading function $l_0(\xi)$ by linearized thin wing theory at the (subsonic) Mach number $M_n = M_0 \cos\phi$ and lift coefficient $C_L \sec^2\phi$; note that $l_0(\xi)$ will differ from the full potential theory loading. These steps are illustrated in Fig. 13. We then take the loading function for our actual three-dimensional wing to be

$$l(\xi) = l_0(\xi) \cos^2\phi \tag{8}$$

The advantage of this procedure can be seen by considering the simpler problem of designing an infinite yawed wing of sweepback ϕ, supposing that we are allowed to use only the techniques of linearized theory. It is clear that the mean camber surface resulting from the choice of loading (8) will be just that required to give the desired section normal to the leading edge, designed by the more powerful methods that are available in two dimensions. It is in fact found in practice that when the method is applied to a finite wing, the shape of the centre portion of each half span turns

out to be almost identical to that of the corresponding infinite wing; the three-dimensional effects occur chiefly as end corrections at the root and tips. Thus there is good reason to hope that in this way some of the more important non-linear effects in the design of the wing camber surface may be allowed for. The load distributions that are arrived at are of the form, standard in two-dimensional thin wing theory

$$l(\xi) = \sqrt{\frac{1-\xi}{\xi}}\,(a_0+a_1\xi+a_2\xi^2+\cdots) \tag{9}$$

Unfortunately, a satisfactory numerical procedure for calculating the full flow field from equation (4) with loadings of this type is not yet available, and up to the present most of the work at supersonic Mach numbers[17,18] has been restricted to simple loadings of the type

$$l(\xi) = a_0+a_1\xi \tag{10}$$

These have the defect that the downwash becomes logarithmically infinite at subsonic leading edges, and so the resulting section shapes are far from ideal. In spite of this, a model designed on these lines has shown that the desired type of flow—with the wings free from shock waves—can in fact be obtained up to a Mach number of 1·2 and a lift coefficient of 0·25, with a wing of aspect ratio 3·5 and 55° sweep; and lift-drag ratios were obtained corresponding to full scale values between 11·5 and 12.

In order to make use of the further improvements which should be obtainable with more general loadings (equation (9)), it is at present necessary to employ the simplified form taken by equation (4) when $M_0 = 1$. With loadings of type (10) it has been found that the wing shapes thus obtained do not vary much with design Mach number in the range $M_0 =$ 1—1·2, so that the simplification should not seriously invalidate the proposed method over this speed range. It is then possible to obtain the upwash w in the wing plane directly in the form

$$w(x,y,o) = \frac{1}{4\pi}\int\limits_{x_1<x}\int \frac{l(x_1,y_1)\,\mathrm{d}x_1\,\mathrm{d}y_1}{(y-y_1)^2} \tag{11}$$

the integral being taken over that part of the (x_1,y_1) plane ahead of the point (x,y,o). Transforming the variables (x_1,y_1) to (ξ,y_1), this becomes

$$w = \frac{1}{4\pi}\int\int \frac{c(y_1)\,l(\xi)\,\mathrm{d}\xi\,\mathrm{d}y_1}{(y-y_1)^2} \tag{12}$$

and integrating this with respect to ξ we obtain

$$w = \frac{1}{4\pi}\int\limits_{-y_l(x)}^{y_l(x)} \frac{c(y_1)\,L(\xi^*)\,\mathrm{d}y_1}{(y-y_1)^2} \tag{13}$$

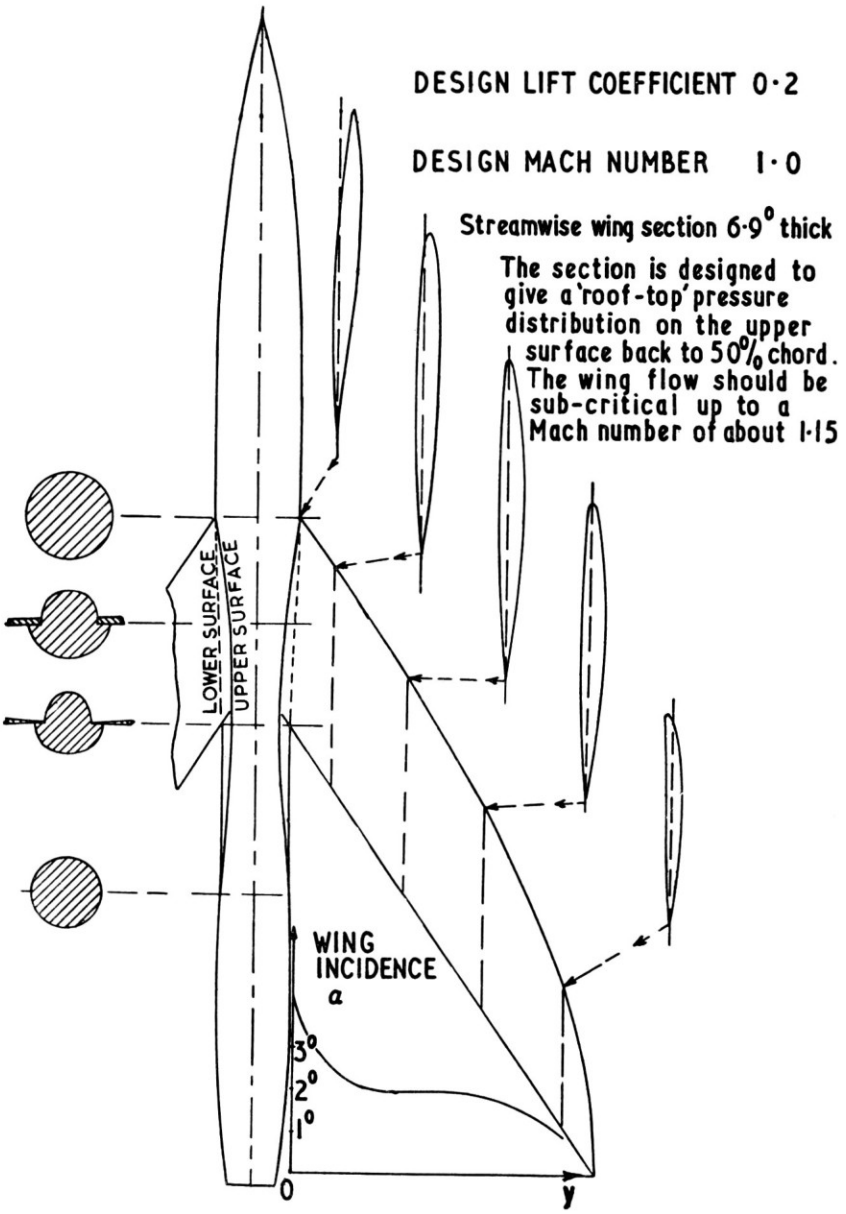

FIG. 15. A typical wing-fuselage design.

where $\xi^*(x, y_1) = \dfrac{x - x_l(y_1)}{c(y_1)}$ is the distance from the leading edge, measured as a fraction of the local chord, of the point (x, y_1, o) and L is defined by equation (7).

This integral (13) is remarkably similar, both in the nature of the singularity in the denominator and in the behaviour of the numerator at the leading edge, to an integral occurring in the subsonic linearized theory of symmetrical aerofoils in two-dimensional flow. It is therefore possible to adapt the method which has been developed by Multhopp and Weber[19] for numerical calculation of the singular integral; this involves only the computation of the numerator in (13) at certain predetermined points along each line $x =$ constant, the corresponding values of w being obtained at the same points by a simple double summation process.

It is not possible to give full details of this process here; but in conclusion we will quote some results that have been obtained for a typical example (Fig. 15). The wing planform corresponds to (C) of Fig. 8, with a basic sweep of 55° and aspect ratio 3·5. The streamwise wing sections are 6·9% thick (12% thick normal to the straight part of the leading edge), and were designed to have a "roof-top" pressure distribution back to 50% chord at the design lift coefficient 0·2. The basic fuselage is cylindrical in the neighbourhood of the wing junction and has a radius equal to one fifth of the wing root chord. Although the design was carried out, as described above, using sonic theory, the pressure distribution on the wing should remain sub-critical up to a Mach number of about 1·15, provided of course that the design method is successful in dealing with the end effects.

The most remarkable feature of the final shape of the wing and fuselage (Fig. 15) is the lack of any extremes of wing warp or fuselage waisting. The relatively small minimum width of the upper half of the fuselage (at the wing trailing edge) would probably present the greatest practical objection to the design, but it is possible that this could be relaxed without serious effects on aerodynamic efficiency, and in any case an increase in wing twist near the root would provide a possible alternative. A model based on this design is being manufactured and will be tested shortly at the National Physical Laboratory as part of an extensive research programme in this field. Later models will be used to investigate the efficacy of some refinements in section design[2] when applied to highly swept wings, and to see how similar ideas can be applied to wings with basically tapered planforms.

ACKNOWLEDGMENT

The work described above has been carried out as part of the research programme of the National Physical Laboratory, and this paper is published by permission of the Director of the Laboratory.

REFERENCES

1. KÜCHEMANN, D., *Aircraft shapes and their aerodynamics for flight at supersonic* speeds. Paper for I.C.A.S. Conference, Zürich, 1960.
2. PEARCEY, H. H., The Design of Wing Sections for Swept Wings at Transonic Speeds. Paper for I.C.A.S. Conference, Zürich, 1960.
3. ROGERS, E. W. E. and HALL, I. M., An Introduction to the Flow about Plane Sweptback Wings at Transonic Speeds, NPL/Aero/394 (January 1960); also in the *J. Roy. Aeronaut. Soc.*, August, 1960.
4. MANGLER, K. W., Calculation of the Pressure Distribution over a Wing at Sonic Speeds, Aeronautical Research Council (London) R. and M. 2888, 1951.
5. MIRELS, H., Aerodynamics of Slender Wings and Wing-body Combinations having Swept Trailing edges. N.A.C.A. Tech. Note 3105, 1954.
6. LOCK, R. C., The Design of Wing Planforms for Transonic Speeds, *A.R.C.* 21, 480, 1959.
7. WHITCOMB, R. T., A Study of the Zero-lift Drag-rise Characteristics of Wing-body Combinations near the Speed of Sound. N.A.C.A. Report 1273, 1956.
8. WHITCOMB, R. T. and FISCHETTI, T. L., Development of a Supersonic Area Rule and an Application to the Design of a Wing-body Combination having High Lift-to-drag ratios. RN.A.C.A. RM L53 H31a, 1953.
9. KÜCHEMANN, D. and HERTLEY, D. E., The Design of Swept Wings and Wing-body Combinations to have Low Drag at Transonic Speeds. R.A.E. Report Aero 2537 1955.
10. BYRD, P. F., Theoretical Pressure Distributions for some Slender Wing-body Combinations at Zero Lift. N.A.C.A. Tech. Note 3674, 1956.
11. MCDEVITT, J. B. and TAYLOR, R. A., An Investigation of Wing-body Juncture Interference Effects at Transonic Speeds for Several Swept-wing and Body Combinations: N.C.A. RM A57 A02, 1957.
12. HAINES, A. B., Wing Section Design for Sweptback wings at Transonic Speeds, *J. Roy. Aeronaut. Soc.*, April 1957.
13. RICHARDSON, J. R. and PARRY, J. T., The Design of Antisymmetric Body Waisting and Camber for Swept and M Wings at Supersonic Speeds, Handley Page unpublished note, 1958.
14. SEARS, W.R. (Ed.), *High Speed Aerodynamics and Jet Propulsion*, Vol. II, pp.148 *et seq.* Princeton, 1955.
15. PALMER, W. E., HOWELL R. R. and BRASLOW, A. L., Transonic Investigation at Lifting Conditions of Streamline Contouring in the Sweptback Wing-fuselage Juncture in Combination with the Transonic Area Rule N.A.C.A. RM L56 D11a, 1956.
16. LOCK, R. C. and ROGERS, E. W. E., Some Preliminary Experimental Results on the Effect of Asymmetric Body Waisting on the Drag due to Lift of a Sweptback Wing at Transonic Speeds. N.P.L. Aero Note 328, 1958.
17. BAGLEY, J. A. and BEASLEY, J. A., The Shapes and Lift-dependent Drag of some Sweptback Wings Designed for M=1·2. R.A.E. Report Aero 2620, 1959.
18. ROPER, G. M., Formulae for Calculating the Camber Surfaces of Thin Sweptback Wings of Arbitrary Planform with Subsonic Leading Edges and Specified Load Distribution. R.A.E. Report Aero 2623 (1959).
19. WEBER, J., The Calculation of the Pressure Distribution over the Surface of Two-dimensional and Swept Wings with Symmetrical Aerofoil Sections. A.R.C. R and M 2918, 1956.
20. WEBER, J., The Shape of the Centre Part of a Sweptback Wing with a Required Load Distribution R.A.E. Report Aero 2591, 1957.